

**ELECTRON TRANSPORT STUDIES IN 12-MER
SINGLE STRAND DNA OLIGOMERS BY MUON
SPETROSCOPY AND SCANNING TUNNELING
MICROSCOPY**

HARISON BINTI ROZAK

UNIVERSITI SAINS MALAYSIA

2021

**ELECTRON TRANSPORT STUDIES IN 12-MER
SINGLE STRAND DNA OLIGOMERS BY MUON
SPETROSCOPY AND SCANNING TUNNELING
MICROSCOPY**

by

HARISON BINTI ROZAK

**Thesis submitted in fulfilment of the requirements
for the degree of
Doctor of Philosophy**

October 2021

ACKNOWLEDGEMENT

First of all, Praise be to Allah s.w.t. because I managed to complete my thesis with the help and contribution a lot of individuals and School of Distance Education, USM. I would like to express my special gratitude to my supervisors, Prof Dr. Shukri Sulaiman and Dr Isao Watanabe for the guidance, support and encouragement in finishing my research and study. I would also like to acknowledge with sincere appreciation to Associate Prof. Kochi Ichimura, for his help in data collection and taught me the methodology to perform STM measurement. My sincere thanks also goes to USM, RIKEN and Hokkaido University for the permission of conducting this research and using the facility to conduct experiment. Last but not least, I would like to thank my parents, family and friends for supporting to complete my research work and thesis.

TABLE OF CONTENTS

ACKNOWLEDGEMENT	ii
TABLE OF CONTENTS	iii
LIST OF TABLES	vi
LIST OF FIGURES	vii
LIST OF SYMBOLS	xi
LIST OF ABBREVIATIONS	xii
LIST OF APPENDICES	xiii
ABSTRAK	xiv
ABSTRACT	xv
CHAPTER 1 INTRODUCTION	1
1.1 Background of Study.....	1
1.2 Problem Statement	5
1.3 Objective of study	5
1.4 Scope of Study	5
1.5 Outline of Study	6
CHAPTER 2 LITERATURE REVIEW	7
2.1 Deoxyribonucleic Acid	7
2.2 Electron Transfer in DNA	9
2.3 Electron Transfer Role in the Biological System.....	10
2.4 Observation of DNA Image by using STM	11
2.5 DNA Conductivity Measurement by Using STM.....	13
2.6 Electron Transfer in DNA Study by Muon Spin Relaxation Technique.....	14
2.7 Risch-Kher Model and 1-Dimension Electron Diffusion	16
2.8 Factors Affecting the Conductivity Measurement in DNA.....	17

CHAPTER 3	METHODOLOGY.....	21
3.1	Introduction	21
3.2	Scanning Tunneling Microscope.....	21
3.2.1	The Working Principle of the STM.....	21
3.2.2	Operational Mode of STM System	23
3.2.3	Experimental Set-Up and Details.....	24
3.2.3(a)	Sample Preparation for STM.....	24
3.2.3(b)	STM Imaging.....	27
3.2.3(c)	Tip-Height Profile Measurements	29
3.2.3(d)	Conductivity Measurement in Different Environments.....	31
3.2.3(e)	Current Voltage Measurements	32
3.3	Muon Spectroscopy.....	33
3.3.1	Properties of Muon.....	33
3.3.2	Basic Principles of Muon Spin Relaxation	35
3.3.3	Probing Electron Transfer in DNA by Electron Labelling Method	39
3.3.4	Muon Experimental Detail and Set-Up.....	41
CHAPTER 4	RESULTS AND DISCUSSION.....	43
4.1	Introduction	43
4.2	Characterization of Sample	43
4.2.1	STM Imaging on ssDNA ₁₂ Oligomer.....	43
4.2.1(a)	Topographic Images	43
4.2.1(b)	Log Current Images	47
4.2.2	Length of Oligomers	49
4.2.3	Width of Oligomers.....	52
4.3	Electron transfer conductivity in ssDNA ₁₂	56
4.3.1	Tip-Height Profile of ssDNA ₁₂ oligomers	57

4.4	Conductivity of ssG ₁₂ in Atmosphere and Vacuum conditions.....	62
4.4.1	Topography Images.....	62
4.4.2	Tip-Height profile	64
4.4.3	Current-Voltage Curve (I-V).....	66
4.5	Characterization of Electron Transfer in ssDNA ₁₂	68
4.5.1	μSR as a Function of Time.....	68
4.5.2	R-K Relaxation Rate Parameter	71
	4.5.2(a) Behaviour of Electron Transfer in ssDNA ₁₂ and dsDNA ₁₂	71
	4.5.2(b) R-K relaxation rate of ssDNA ₁₂ oligomers.....	75
	CHAPTER 5 CONCLUSION AND FUTURE WORK	77
5.1	Conclusion.....	77
5.2	Future Work	78
	REFERENCES	79
	APPENDICES	
	LIST OF PUBLICATION	
	LIST OF PRESENTATION	

LIST OF TABLES

	Page
Table 1.1 Sequences of ssDNA ₁₂ samples	4
Table 3.1 Basic properties of the positive muon (μ^+) [66]	34
Table 4.1 Comparison between mean \pm SD of the length of ssG ₁₂ , ssC ₁₂ , ssA ₁₂ , and ssT ₁₂ oligomers	52
Table 4.2 Comparison between mean \pm SD of the width for ssG ₁₂ , ssC ₁₂ , ssA ₁₂ , and ssT ₁₂ oligomers	55
Table 4.3 Comparison between mean \pm SD of the tip-height profile of ssG ₁₂ , ssC ₁₂ , ssA ₁₂ , and ssT ₁₂ oligomers.....	60

LIST OF FIGURES

	Page
Figure 1.1	Schematic images of two mechanisms of electron transport (a) tunneling and (b) hopping [21].2
Figure 2.1	Four different types of the nitrogenous base in DNA 7
Figure 2.2	Structure of dsDNA with its stacked base pairs that are linked together with the sugar-phosphate backbone.8
Figure 2.3	Structure of double-helix DNA with its stacked base pairs and atomic π_z orbitals perpendicular to the stacked base pairs [1].9
Figure 2.4	Model of electron transfer through DNA to detect and repair the damaged site in DNA [42]. 10
Figure 2.5	STM image of dsDNA on the flat graphite substrate [44] 11
Figure 2.6	Image of ssDNA oligomer on the Cu (111) substrate [48]..... 12
Figure 2.7	STM image of ssDNA consist of ACTG bases. The brightest one is the guanine bases [49] 12
Figure 2.8	I-V spectra of dsAT and dsGC [32]..... 13
Figure 2.9	I-V spectra of ssMIX and dsMIX sequences. This curve was measured at a set point of 0.1 nA and 0.1 V [32]..... 14
Figure 2.10	Magnetic field dependence of relaxation rate spectra fitted using the R-K power-law fitting function [37]. 15
Figure 2.11	Field dependence of the integrated asymmetry for ssDNA and dsDNA that was measured at 5K [51]..... 16
Figure 2.12	Log current imaged and I-V spectra of DNA that was measured under dry condition [38]..... 19
Figure 2.13	I-V characteristic of DNA measured by STM [28]20
Figure 3.1	Schematic image of the pathway of electron tunneling from the occupied tip states to the unoccupied sample states, (a) before tip

	approaching the sample, (b) after the tip approaching the sample surface.	22
Figure 3.2	Operational modes in the STM system (a) constant height mode (b) constant current mode.....	24
Figure 3.3	STM image of sample preparation (a) Pt-Ir STM tip and (b) HOPG substrate taken using a microscope. (c) Cleaning process of HOPG substrate.....	26
Figure 3.4	The images of (a) a droplet of the sample solution on the graphite substrate. (b) The sample solution was kept in a petri dish that contains silica gel for the dry-up process.....	26
Figure 3.5	Basic set up of STM machine (JSPM-5200, JEOL, Japan)	27
Figure 3.6	WinSPM for scanning probe microscope. The control software to perform STM measurement	28
Figure 3.7	The image of oligomers on the graphite substrate that measured in the different scan area (a) $1\ \mu\text{m} \times 1\ \mu\text{m}$, (b) $0.4\ \mu\text{m} \times 0.4\ \mu\text{m}$, (c) $0.2\ \mu\text{m} \times 0.2\ \mu\text{m}$, and (d) $0.04\ \mu\text{m} \times 0.04\ \mu\text{m}$. The red circle indicated the possible location of oligomers.....	29
Figure 3.8	Schematic images of the pathway of electron transfer from the tip to the sample. (a) conductive sample and (b) less conductive sample	31
Figure 3.9	Green cross marker in the topographic image indicates the location that chose for I-V measurement	33
Figure 3.10	Illustration of muon production process	35
Figure 3.11	Decay of the muon into a positron and a pair of neutrinos [67]	35
Figure 3.12	The angular distribution of distributed positron [68].....	36
Figure 3.13	(a)The time histogram of accumulated positron counted by forward and backward counter. (b) The time dependence of an asymmetry measured in a TF condition [68].	37
Figure 3.14	Position of positron detector in the set up μSR measurement (a) parallel to muon beam (b) antiparallel to muon beam [67].....	38

Figure 3.15	Electron labelling method process.	40
Figure 3.16	Experimental set up for μ SR measurements on ssDNA ₁₂ samples. (a) sample was wrapped in a silver package in the form of a pallet, (b) mounted sample on a mini cryostat, (c) ARGUS spectrometer, (d) mini cryostat was loaded into the Argus spectrometer.....	42
Figure 4.1	3D-topography images of ssDNA ₁₂ oligomers (a) ssG ₁₂ , (b) ssC ₁₂ , (c) ssA ₁₂ , and (d) ssT ₁₂ aligned in parallel to each other and formed a one-dimensional (1D) chain structure on the flat graphite substrate.....	45
Figure 4.2	2D log-current images of ssDNA ₁₂ oligomers (a) ssG ₁₂ , (b) ssC ₁₂ , (c) ssA ₁₂ , and (d) ssT ₁₂ aligned in parallel to each other and formed a one-dimensional (1D) chain structure on the flat graphite substrate.....	48
Figure 4.3	Analyses s of length for ssDNA ₁₂ oligomers (a) ssG ₁₂ , (b) ssC ₁₂ , (c) ssA ₁₂ , and (d) ssT ₁₂	50
Figure 4.4	Width analyses for ssDNA ₁₂ oligomers (a) ssG ₁₂ , (b) ssC ₁₂ , (c) ssA ₁₂ , and (d) ssT ₁₂	53
Figure 4.5	3D-topography images with details mean \pm (SD) of the width and length for ssDNA ₁₂ oligomers (a) ssG ₁₂ , (b) ssC ₁₂ , (c) ssA ₁₂ , and (d) ssT ₁₂	55
Figure 4.6	Analyses of the tip-height profile spectra for ssDNA ₁₂ oligomers (a) ssG ₁₂ , (b) ssC ₁₂ , (c) ssA ₁₂ , and (d) ssT ₁₂	58
Figure 4.7	The 3D-topography images of (a) graphite substrate that was measured under atmosphere condition. (b) ssG ₁₂ oligomer in the atmosphere condition, and (c) ssG ₁₂ oligomer in the vacuum condition.....	62
Figure 4.8	Analysis of tip-height profile spectra of ssG ₁₂ oligomer (a) in the atmosphere condition (b) in the vacuum condition.....	65
Figure 4.9	Topography images of ssG ₁₂ oligomer (a) in the atmosphere condition (b) in the vacuum condition. (c) the I-V curves (d) dI/dV curves of ssG ₁₂ oligomer in both conditions.....	66

Figure 4.10	Muon asymmetry spectra of ssDNA ₁₂ oligomers	69
Figure 4.11	Field dependence of the RK relaxation rate for ssDNA ₁₂ . The solid line is the result of the R-K power law fitting with the critical exponential value, β	72
Figure 4.12	Field dependence of the RK relaxation rate for dsDNA (dsGC ₁₂). The solid line is the result of the R-K power-law fitting with the critical exponential value, β	73
Figure 4.13	ssG ₁₂ oligomer structure was optimized using semi empirical method PM6 [92].	74
Figure 4.14	Structure of dsDNA (dsGC ₁₂) from DFT calculation [92].	75
Figure 4.15	Field dependence of the RK relaxation rate parameter for ssG ₁₂ , ssC ₁₂ , ssA ₁₂ , and ssT ₁₂ oligomers.	76

LIST OF SYMBOLS

θ	Angle
a	Asymmetry parameter
α	Experimental factor
B_{ext}	Externally applied magnetic field
m	Free-electron mass
$\gamma_{\mu} / 2\pi$	Gyromagnetic ratio
Γ_{μ}	Lifetime
ρ_s	Local density of states of sample
ρ_t	Local density of states of STM tip
μ_{μ}	Magnetic moment
m_{μ}	Mass
λ_{μ}	Muon spin-relaxation rate
ν	Neutrinos
n	Neutrons
1D	one-dimensional
ϕ_{det}	Phase factor
π	Pion
\hbar	Planck's constant
\hbar	Planck's constant
μ^+	Positive muon
e^+	Positron
p	Protons
S_{μ}	Spin
$P(t)$	Time dependence of the muon-spin polarization
H_p	Tip-height profile
ϕ_s	Work function of the sample
ϕ_t	Work function of the tip
$A(t)$	μ SR time spectrum

LIST OF ABBREVIATIONS

ssA ₁₂	12-mer single strand adenine
ssC ₁₂	12-mer single strand cytosine
ssG ₁₂	12-mer single strand guanine
ssT ₁₂	12-mer single strand thymine
ssDNA ₁₂	12-mer single-strand synthetic DNA
NB	Backward detector
CT	Charge transport
I	Current
DFT	Density functional theory
DNA	Deoxyribonucleic acid
dsDNA	Double strand deoxyribonucleic acid
ET	Electron transport
EndoIII	Endonuclease III
NF	Forward detector
HOMO	Highest occupied molecular orbital
4Fe4S	Iron-sulfur clusters
G	Gauss
LF- μ SR	Longitudinal field muon spin relaxation
LUMO	Lowest unoccupied molecular orbital
μ	Muon
μ SR	Muon spin relaxation
STM	Scanning tunnelling microscope
Ag	Silver
ssDNA	Single strand deoxyribonucleic acid
H _p	Tip-height profile
TF- μ SR	Transverse field muon spin relaxation
V	Voltage

LIST OF APPENDICES

Appendix A STM IMAGES

**KAJIAN TERHADAP PERGERAKKAN ELEKTRON DI DALAM
OLIGOMER DNA BEBENANG TUNGGAL 12-MER DENGAN
MENGUNAKAN SPEKTROSKOPI MUON DAN MIKROSKOPI
PENGIMBASAN TEROWONG**

ABSTRAK

Tujuan kajian ini adalah untuk menentukan yang mana antara empat sampel bebenang tunggal 12-mer DNA (ssDNA₁₂) yang paling konduktif dan kurang konduktif. Selain itu, untuk mengetahui sifat pergerakan elektron di dalam sampel ini. Pengukuran mikroskop pengimbasan terowong (STM) dan relaksasi putaran muon (μ SR) dilakukan untuk mencapai objektif kajian. Teknik STM juga digunakan untuk menentukan bentuk setiap oligomer dan untuk mengkaji pengaruh keadaan persekitaran terhadap pengukuran kekonduksian. Dari pengukuran STM, setiap pangkalan dalam DNA didapati konduktif, dan pangkalan yang paling konduktif adalah ssG₁₂. Urutan kekonduksian berdasarkan pengukuran profil ketinggian jarum (H_p) adalah ssG₁₂ > ssC₁₂ > ssA₁₂ > ssT₁₂. Bentuk oligomer dilihat berbeza antara satu sama lain kerana sampel ssDNA₁₂ (ssA₁₂, ssC₁₂, ssG₁₂, and ssT₁₂) adalah struktur yang fleksibel kerana ia terbentuk tanpa pangkalan dan bebenang yang lengkap. Oligomer ini juga dilihat sejajar antara satu sama lain dan membentuk struktur rantai satu dimensi (1D). Teknik μ SR berjaya mengesan kewujudan pemindahan elektron dalam ssDNA₁₂. Pada suhu bilik tingkah laku pemindahan elektron sepanjang ssDNA₁₂ disarankan pada kuasi-1D. Dari pengukuran kekonduksian pada ssG₁₂ di dalam keadaan persekitaran yang berbeza kami dapati kekonduksian tidak bergantung pada persekitaran. Secara keseluruhan, ia dapat disarankan bahawa ssDNA₁₂ itu sendiri bersifat konduktiv dan boleh menjadi ruang untuk pergerakan elektron.

**ELECTRON TRANSPORT STUDIES IN 12-MER SINGLE STRAND DNA
OLIGOMERS BY MUON SPETROSCOPY AND SCANNING TUNNELING
MICROSCOPY**

ABSTRACT

The aims of this study are to determine which of the four samples of 12-mer single-strand: adenine, cytosine, guanine, and thymine (ssA₁₂, ssC₁₂, ssG₁₂, and ssT₁₂) is the most and least conductive. Besides, to find out the behaviour of the electron transfer in these samples. Scanning tunneling microscope (STM) and muon spin relaxation (μ SR) measurements were performed to achieve the objectives study. The STM technique was also used to determine the shape of each oligomer sample and to study the influence of environmental conditions on the conductivity measurement. From STM measurements, each base in DNA was found to be conductive, and the most conductive base is ssG₁₂. The sequence of conductivity based on the tip-height profile (H_p) measurement is ssG₁₂ > ssC₁₂ > ssA₁₂ > ssT₁₂. The shapes of oligomers were observed to be different from each other because ssDNA₁₂ samples (ssA₁₂, ssC₁₂, ssG₁₂, and ssT₁₂) are flexible structures as they are formed without any complement bases and strand. These oligomers were also seen aligned in parallel from each other and formed a one-dimensional (1D) chain structure. The μ SR technique successfully detected the existence of electron transfer in ssDNA₁₂. The behaviour of the electron transfer along the ssDNA₁₂ was suggested in quasi-1D at room temperature. From conductivity measurement in different environment conditions on ssG₁₂, it was found that conductivity did not depend on the environmental conditions. Overall, it can be suggested that ssDNA₁₂ itself is conductive and they can be a medium for the electron to transfer.

CHAPTER 1

INTRODUCTION

1.1 Background of Study

Deoxyribonucleic acid (DNA) is considered the blueprint of life because it contains all the instructions for cells to grow and function [1]. It is a macromolecule that consisting of four nucleotide bases: adenine (A), cytosine (C), guanine (G) and thymine (T) attached to a sugar and phosphate group [2]. DNA has received a lot of attention over the past few decades due to DNA remarkable feature which is π - π stacking interaction between the aromatic ring of DNA nucleobase [1, 3, 4]. This feature has opened a possibility for the migration of electron or electron transport (ET) in DNA [1, 4].

The ET phenomenon has generated a lot of interest among physicists, biologists, and chemists. In the biological field, ET is believed to play an important role in the biological process. For instance, the processes of damaged and repair mechanism in DNA, transcription factors and/or polymerase cofactor [5-13]. Besides that, the conductivity of ET in DNA can open a possibility to use DNA as nano-electronic devices [14-16]and biomedical sensors [17-19]. Therefore, a deeper understanding of the ET process in DNA is essential to study especially at the microscopic level.

Numerous studies have been carried out to investigate and explore the existence of the ET process in the DNA [20-25]. In 2002, Boon and Barton [21] have been proposed that there are two mechanisms of electron transfer/transport in DNA namely hopping and tunneling, as shown in Figure 1.1 (a) and Figure 1.1 (b), respectively. In the hopping mechanism, the electron is hopping between the π - π stacked DNA base pairs, and the electron is localized on the bases and exchanges the

energy [22, 23]. This hopping mechanism can transfer for long distances. In the tunneling mechanism, electron tunnels from the donor to the acceptor without exchange the energy with the DNA bases [24, 25]. Unlike the hopping mechanism, the tunneling mechanism can transfer the electron over a short distance.

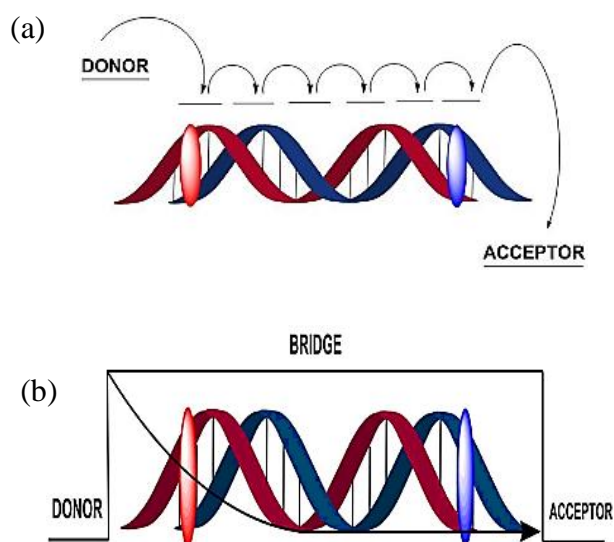


Figure 1.1 Schematic images of two mechanisms of electron transport (a) tunneling and (b) hopping [21].

lots of experimental studies have been carried out to investigate the conductivity of DNA [26-30]. Some studies found that DNA is an insulator [26, 27], a semiconductor [28, 29] or a simple metallic conductor [30]. These findings have emerged the confusion until now because if DNA is an insulator DNA could not be a medium for the electrons to transfer. The potential factors of these inconsistent findings might be contributed by the difference in DNA sequence [31, 32] the variation of its medium or environments (wet or dry) [33, 34], and the length of the DNA sequence that was used in the research studies [35, 36].

Torikai et al. [20] and Nagamine et al [37] have found the existence of ET in DNA by using muon spin relaxation (μ SR) spectroscopy technique. The μ SR measurements were performed on A form DNA (with 30 % water molecule) and B

form DNA (with 50 % water molecule) conditions. Torikai et al. [20] and Nagamine et al. [37] demonstrated that ET in one-dimensional (1D) and quasi-1D through A and B forms DNA. In addition, ET through DNA strand was proposed more enhanced in the drier and more densely packed A-form DNA compared to the B-form DNA. However, the electron diffusion rate and DNA conductivity were not discussed in these papers probably due to the huge and unknown sequence of nucleobase in these DNA samples. Torikai et al. [20] and Nagamine et al. [37] measured real DNA molecules extracted from the Herring Sperm. Accordingly, it was almost impossible to know the location of stopping muon in DNA and to quantitatively discuss the conductivity, and diffusion rate of the electron in DNA [20, 37].

Besides, Terawaki et al. [34] carried out the scanning tunnelling microscope (STM) measurement on DNA and reported that DNA is not conductive. Electrical conductivity of DNA was measured under the dry (with 0 % moisture) and wet (with 60 % moisture) conditions. This study proposed that electrical current of DNA only can be measured under wet condition due to the contribution of ionic conduction through water layers that surrounded the DNA while the electrical current cannot be measured under dry condition. On the other hand, Sharipov et al. [28] and Duli et al. [33] found that in a dry condition DNA is not an insulator and exhibit conductivity property. While Xu et al. [38] results, revealed that the conductivity of DNA is not contributed by the ionic conduction mechanism in wet conditions.

Based on these previous studies [28-38], an important question arises as to whether DNA is conductive or not. and which of the four bases in DNA (guanine (G), cytosine (C), adenine (A), and thymine (T)) is the most and the less conductive one. The next research question is the behaviour of electron transfer is different in each sequence of DNA strand. Furthermore, the following question is to address the issue

of whether the environmental conditions (humid or dry) will affect the DNA conductivity measurements. For instance, will humid condition influence the conductivity measurements in DNA by inducing an ionic conduction mechanism.

To address these research questions, firstly, we need to understand the electron transfer process in each four nucleotide bases DNA. Therefore, the ET in DNA was systematically studied by using various forms of DNA samples. These samples are different from the previous studies by Nagamine et al. [37], Xu et al. [38], Terawaki et al. [34], Duli et al.[33], and Sharipov et al.[28], in which previous samples are consisted of dsDNA that contains random bases. The bases in these samples can be either guanine (G), adenine (A), cytosine (C), or thymine (T) attached to the sugar-phosphate backbone. Hence, it is almost impossible to know which bases in DNA samples is conductive or not.

Accordingly, samples were designed much simpler than the dsDNA. The samples consist of 12-mer single-stranded synthetic DNA (ssDNA₁₂), and each strand has only one type of base. The ssDNA₁₂ samples has been tabulated in Table 1.1

Table 1.1 Sequences of ssDNA₁₂ samples

Code	Name	Sequences
1	ssA ₁₂	5'-AAAA AAAA AAAA- 3'
2	ssC ₁₂	5'-CCCC CCCC CCCC- 3'
3	ssT ₁₂	5'-TTTT TTTT TTTT- 3'
4	ssG ₁₂	5'-GGGG GGGG GGGG- 3'

1.2 Problem Statement

In the past years, much attention has been paid to the ET process in dsDNA due to the fundamental role of ET in the biological process and the prospect to be used as nanoelectronics devices. However, until now, the fundamental process of DNA conductivity [28, 34, 38] and the behaviour of electron transfer in dsDNA [20, 37] is still remain unknown. Hence, to understand the complex process of electron transfer in dsDNA, a systematic study of the electron transfer in ssDNA₁₂ is required to set the baseline readings of electron transfer in each four nucleotide bases DNA and to open a new perspective for understanding the detail of this process.

1.3 Objective of study

Generally, the main purpose of this research was to study the electron transport process in dsDNA and its electronic properties. To clarify these issues at the first stage, we need to understand the electron transport process on the basic ssDNA₁₂ first. Thus, the objectives of this thesis are:

- i. To characterize the behaviour of electron transfer of ssDNA₁₂ samples (ssG₁₂, ssC₁₂, ssA₁₂ and ssT₁₂) with varying external magnetic field using muon spin relaxation technique
- ii. To determine the order of electron conductivity in four ssDNA₁₂ samples (ssG₁₂, ssC₁₂, ssA₁₂ and ssT₁₂) using scanning tunneling microscopy
- iii. To determine the effect of atmospheric humidity on the electron conductivity in ssG₁₂ oligomers using scanning tunneling microscopy

1.4 Scope of Study

This study was focused on the muon spin relaxation measurements of these four samples (ssG₁₂, ssC₁₂, ssA₁₂ and ssT₁₂) at room temperature to study the behaviour

of electron transfer. The electron diffusion rate was not included due to limited muon beam time facility at RIKEN-RAL United Kingdom.

For STM measurements, tip-height profile and topographic images of all oligomers were measured. Due to limited access of the STM facility at Hokkaido University, electrical current measurements are conducted only on ssG₁₂ sample.

1.5 Outline of Study

This thesis consists of five chapters. In Chapter 1, the background of this study is discussed, and it introduces the structure of DNA and the importance of the electron transport process in DNA for the biological phenomenon. It also presented the objectives to be accomplished, the problem statement, and the scope of the study. In Chapter 2, the results of the previous studies related to the topic of this work are presented. Chapter 3 is all about instruments, materials, and procedures that used in this study. Chapter 4 presents the results and discussion that acquired from the measurements. Finally, Chapter 5, this chapter explained the conclusion and summary of the study, along with future recommendations for future research.

CHAPTER 2

LITERATURE REVIEW

2.1 Deoxyribonucleic Acid

DNA is the molecule that contains all the information for our cell to grow and function. It is formed using sequences of four nitrogenous bases, which can be either adenine (A), thymine (T), guanine (G), or cytosine (C), attached to a sugar molecule and a phosphate backbone [39].

The main difference between these bases is the structure of bases in which guanine and adenine have double rings (purine ring) structure. Meanwhile, cytosine and thymine have a single ring (pyrimidine ring) as demonstrated in Figure 2.1.

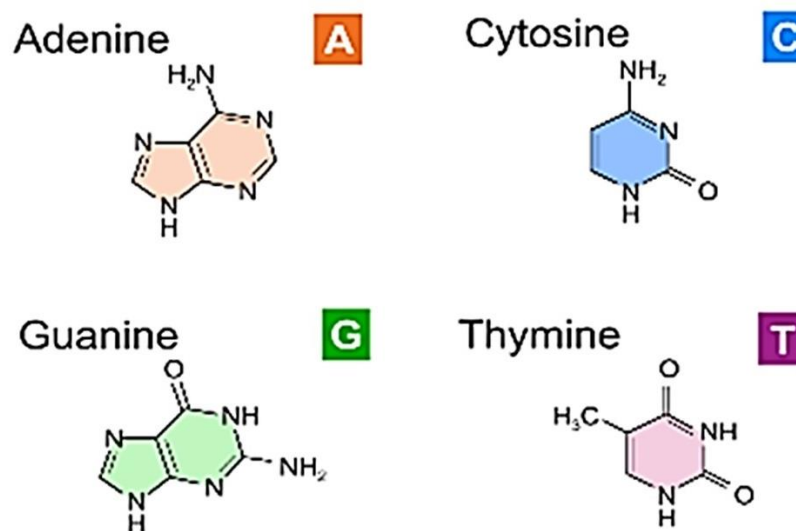


Figure 2.1 Four different types of the nitrogenous base in DNA

The main difference between the nitrogenous bases of DNA is the guanine base contains one amine group, one carbonyl group, and three double bonds in its pyrimidine ring, whereas the adenine base consists of an additional double bond and one amine group. The cytosine base, it contains one amine group, one keto group, and

two double bonds, and the thymine base contains two keto groups and one methyl group in its pyrimidine ring, as shown in Figure 2.1.

The structure of the dsDNA is made of two linear strands of repeating sugar molecules and phosphate groups that twisted around each other. These two linear strands of double-helix DNA are held via hydrogen bonds in which connected to the bases of DNA. Adenine pair with thymine and cytosine pair with guanine as demonstrated in Figure 2.2. The width of DNA is about 2 nm, and for about ten base pairs (bp), the length of double-helix DNA is about 3.4 nm [40]. Generally, the length of real dsDNA can be up to several meters and its form as a worm-like-chain polymer.

Single-strand DNA (ssDNA) is formed of a sugar-phosphate backbone that linking together either with A, C, T, or G bases without the base pairing and complement strand [2]. The ssDNA is used to be known as a flexible and less stiff molecule than the dsDNA. Accordingly, it can fold up into a variety of shapes.

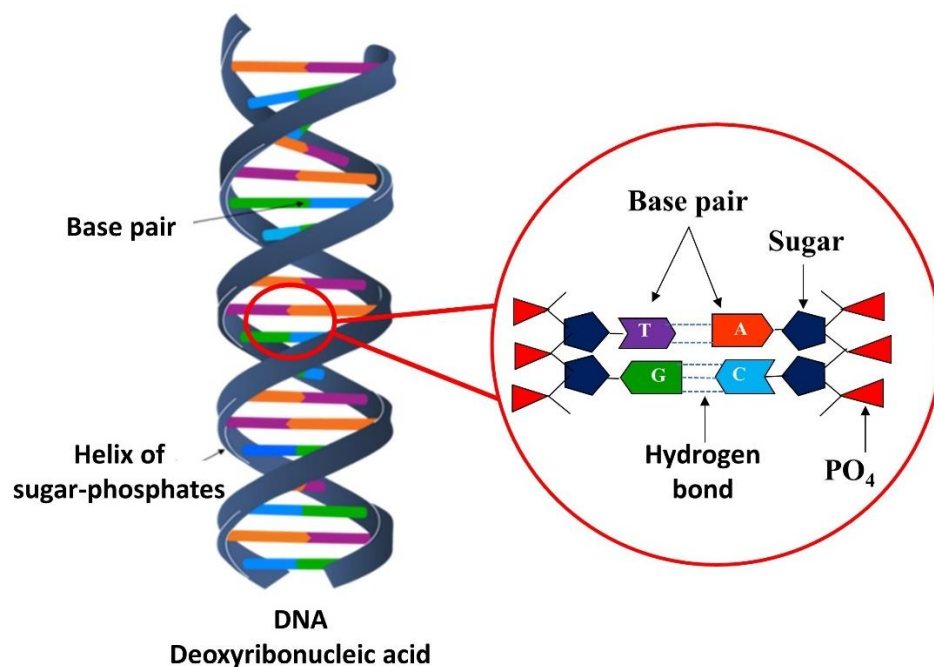


Figure 2.2 Structure of dsDNA with its stacked base pairs that are linked together with the sugar-phosphate backbone.

2.2 Electron Transfer in DNA

DNA bases have a hexagonal structure like a benzene ring, and it contains π_z orbitals. Whenever atomic π_z orbitals perpendicular to the plane of the adjacent DNA bases, the π bonding and π^* antibonding will be formed as shown in Figure 2.3 [1]. These π - π stacking could provide a pathway for the electron to transfer. The reason behind this idea is the overlapping of electron clouds or wavefunction of the stacked base pairs [41]. If the π - π stacking between the base pairs is strong enough, it causes the energy gap to become smaller, and the DNA structure becomes more conductive.

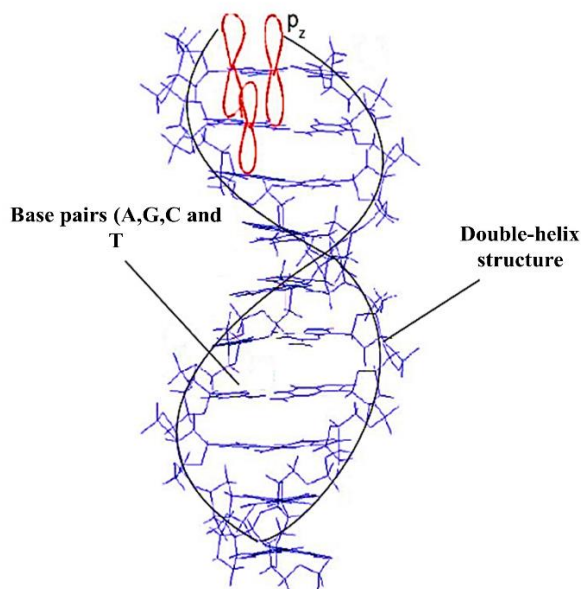


Figure 2.3 Structure of double-helix DNA with its stacked base pairs and atomic π_z orbitals perpendicular to the stacked base pairs [1].

2.3 Electron Transfer Role in the Biological System

In the year 2003, Boon et al. [5] proposed that the iron-sulfur [4Fe4S] clusters in base excision repair protein may play an important role in searching the spot of the damage in DNA and repairing damages on it. Some studies have been suggested a model of the DNA damage search and repair process based on these redox-active [4Fe4S] clusters [4, 18, 42, 43]. Figure 2.4 shows how DNA repair protein use DNA-

mediated charge transfer as a means of signaling to locate and repair damaged. Upon DNA repair-protein like Endo III attached to DNA, it changes its [4Fe4S] clusters configuration from 2^+ oxidation state (purple) to 3^+ state (turquoise). If there is no damage in the DNA strand, Endo III must be free to transfer and send electron via charge transfer (yellow arrows) along the molecule to the next recipient Endo III which has a 3^+ state. The successful electron transfer will change the configuration of recipient Endo III from 3^+ to 2^+ . If there is damaged intervening on DNA, the electron cannot pass through the strand, and Endo III will keep binding to the DNA strand to repair the DNA damage.

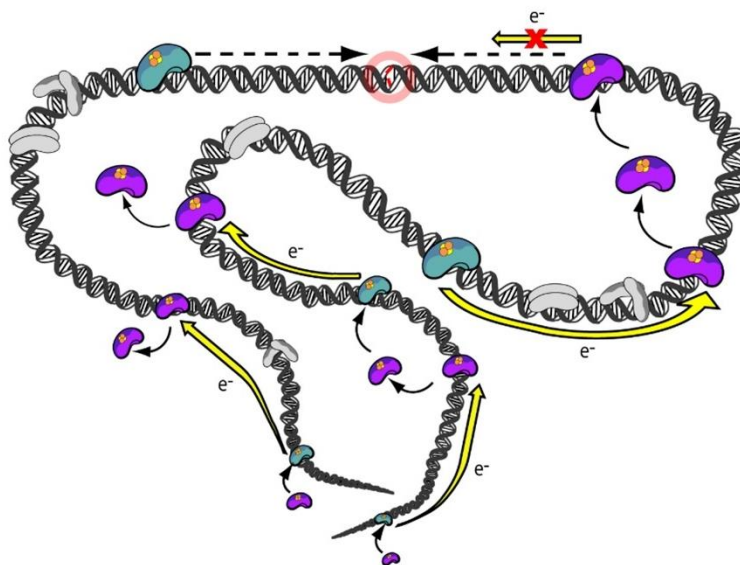


Figure 2.4 Model of electron transfer through DNA to detect and repair the damaged site in DNA [42].

Boal et al. [43] and Grodick et al. [42] have performed measurements by using atomic force microscopy (AFM) to monitor the relation between Endo III and damaged DNA. Endo III was incubated with normal DNA (1900 base pairs) and damaged DNA (3800 base pairs). Boal et al. [43] have found that higher density of Endo III is apparent on the damaged DNA compared to the normal DNA. This measurement shows that

repair protein of Endo III with [4Fe4S] cluster plays a role as a DNA mediated redox signalling [43].

2.4 Observation of DNA Image by using STM

Since the year 1989, the scanning tunneling microscopy technique has already proven to be one of the important techniques to probe the structure of DNA at the atomic level [44 - 46] and to investigate the electrical conductivity of material [32, 35]. Beebe et al. [44] show that the dsDNA structure on the graphite substrate was successfully observed at constant current mode, as shown in Figure 2.5. The images of the helical conformation of dsDNA were appeared much brighter than the graphite substrate, and it indicated that DNA had higher electrical conductivity than the graphite [44].

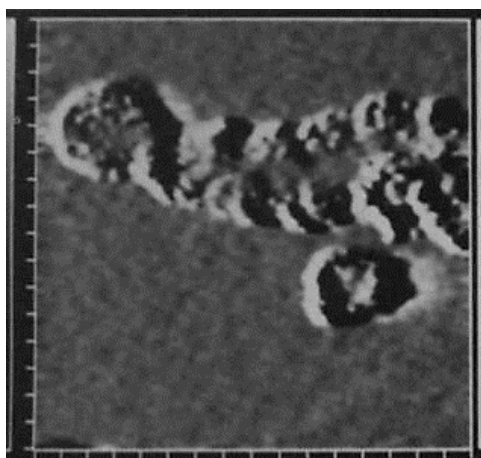


Figure 2.5 STM image of dsDNA on the flat graphite substrate [44]

In 1991, Cricenti et al. [47] revealed that the image of a single base in DNA was not easy to visualize either due to poor local resolution of the tip or due to twisting of the DNA bases. Despite this matter, the images of ssDNA was observable, but only the rough structure of ssDNA.

In 1999, Tanaka et al. [48] conducted measurements on ssDNA and dsDNA using ultra-high vacuum STM at room temperature where the shape of 14-mer ssDNA was found to resemble Z-shape on the copper substrate, as illustrated in Figure 2.6. The width of the DNA sample was observed to be about 2 to 4 nm.

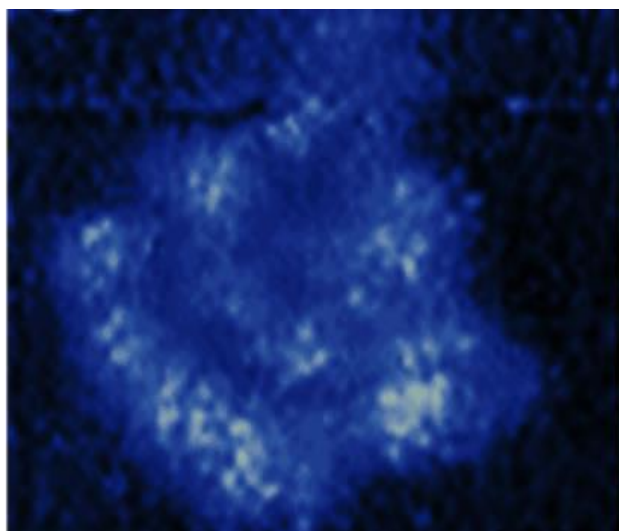


Figure 2.6 Image of ssDNA oligomer on the Cu (111) substrate [48].

In 2009, Tanaka and Kawai [49] carried out STM measurements on a long ssDNA (7249 bases). The study shows that guanine base is the easiest to be detected since it shows a brighter contrast of topographic image compared to the other bases. It was proposed that guanine has the lowest ionization potential of the four bases in DNA [49].

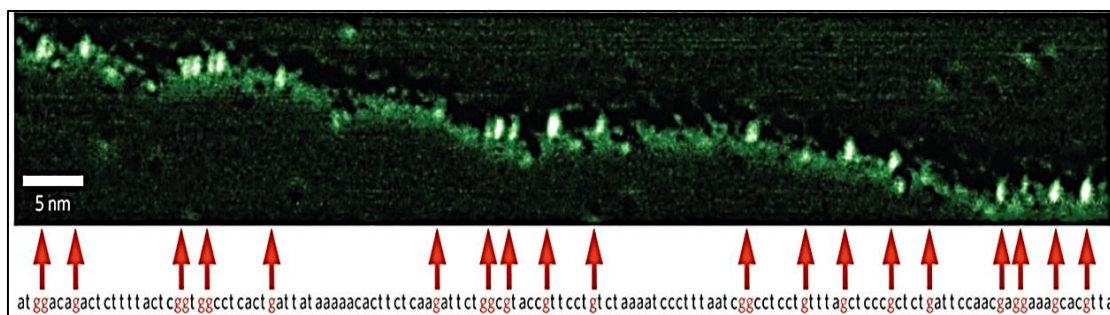


Figure 2.7 STM image of ssDNA consist of ACTG bases. The brightest one is the guanine bases [49].

2.5 DNA Conductivity Measurement by Using STM

In 2008, Kratochvílová et al. [32] measured the conductivity of DNA using STM technique. The DNA samples used in this study consisted of various sequences of ssDNA and dsDNA. Each of the sequences contains 32 bases, and it was chemically modified in order to attach the oligonucleotides with the Au electrode. The I-V curves were collected for several oligonucleotide sequences under ambient conditions. The setpoint parameters of these I-V measurements consisted of 0.1 nA and 0.1 V.

Based on the outcomes of the I-V measurements, Kratochvílová et al. [32] reported that ds GC is more conductive than the dsDNA that contains adenine and thymine bases, as shown in Figure 2.8. The reason behind these results because guanine is known to be an easily oxidized base from the theoretical work [32]. The lower ionization potential of guanine makes it possible and much easier to generate as a charge carrier hole. Then, hopping charge transport would occur, and due to this factor, ds GC was found to be more conductive than ds AT.

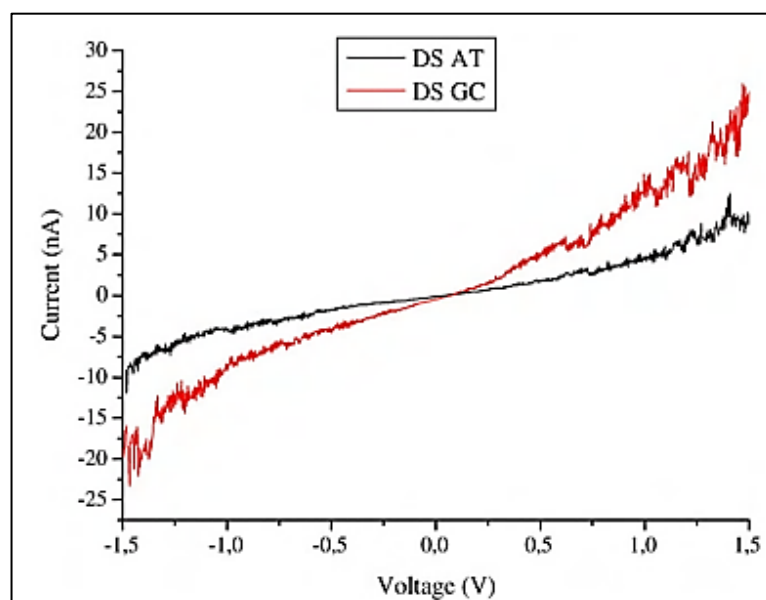


Figure 2.8 I-V spectra of dsAT and dsGC [32]

Besides that, Kratochvílová et al. [32] also revealed that the conductivity of dsDNA is higher than ssDNA due to the base pair stacking and arrangement. This finding shows a good agreement with the theoretical model system, in which ssDNA considers less structural regular than the dsDNA because of base-pair helical arrangements in DNA. The less structural of ssDNA was suggested to decrease the potential overlap of the π - electron system. In the end, Kratochvílová et al. [32] considered that this factor would be caused dsDNA is more conductive than the ssDNA. Figure 2.9 shows the I-V curve of mixed sequences of ssDNA and dsDNA. These sequences have 32 bases mixed with G, C, A, and T.

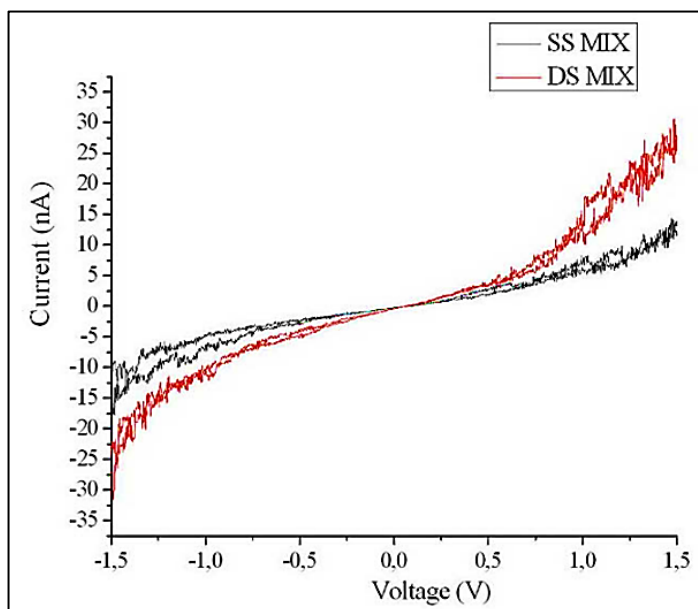


Figure 2.9 I-V spectra of ssMIX and dsMIX sequences. This curve was measured at a set point of 0.1 nA and 0.1 V [32].

2.6 Electron Transfer in DNA Study by Muon Spin Relaxation Technique

Nagamine et al. [50] have successfully established a method utilizing μ SR spectroscopy to observe the microscopic aspects of electron transfer in life science like cytochrome c and myoglobin. In the year 2001, Torikai et al. [37] were performed μ SR measurements on DNA samples by using labelling electron method. The DNA samples

consisted of A-form DNA (30% of a water molecule) and B-form (50% of a water molecule) DNA, and the measurements were measured at room temperature.

Based on the muon spin relaxation on the inverse magnetic field between 80 and 4000 G data, a clear electron transfer signal was directly detected in each sample, and these results indicated a strong influence of the different structural conformations. These results were fitted using the R-K power-law fitting function, and some aspect of one-dimensional (1D) and quasi-one-dimensional (1D) of electron transfer along both strands of A and B forms DNA were observed as shown in Figure 2.10 [20, 37]. Besides that, the electron transfer along the DNA strand is enhanced in the drier and more densely packed A-form DNA compared to the B-form DNA. This is because in B-form DNA, the adjacent base pairs are separated due to a higher level of water content in the DNA environment.

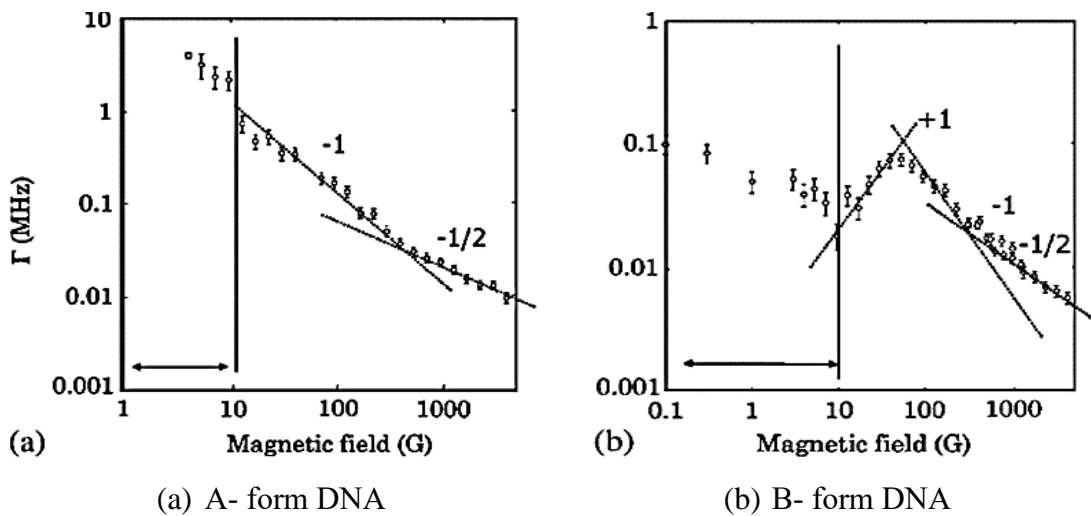


Figure 2.10 Magnetic field dependence of relaxation rate spectra fitted using the R-K power-law fitting function [37].

In 2006, Hubbard et al. [51] conducted μ SR measurements on dsDNA and ssDNA samples to observe the response of muon in different structures. This study reported that integrated asymmetry for dsDNA and ssDNA are different from each other due to the difference in the base-pair arrangement in each sample. Figure 2.11

shows the integrated asymmetry of dsDNA and ssDNA which measured from 0 mT to 100 mT [51].

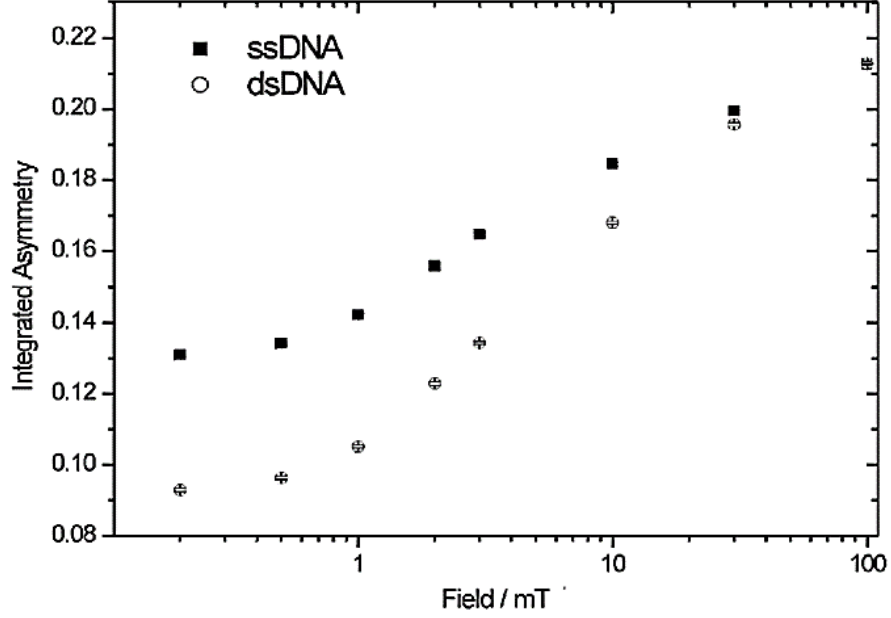


Figure 2.11 Field dependence of the integrated asymmetry for ssDNA and dsDNA that was measured at 5K [51].

2.7 Risch-Kher Model and 1-Dimension Electron Diffusion

Risch-Kher (RK) model was adopted to the muon analysis to study the model of electron transfer on conductive polymer [52, 53]. The RK theory was considered as an appropriate theory to study the 1D model of electron transfer since the time range for the electron to transfer along the chain is longer than the exponential function. In RK, $\lambda t_{max} \gg 1$, where λ is the electron spin-flip rate and t_{max} is the time scale of experiment [54]. For finite longitudinal field (LF), RK predicts the relaxation of the muon spin resulting from interaction with an electron can be modeled using a relaxation function of the form [37].

$$P(t) = \exp[\Gamma(B)t] \operatorname{erfc}\{[\Gamma(B)t]\}^2 \quad (2.1)$$

Where $\Gamma(B)$ is the R-K relaxation parameter-dependent of the magnetic field, t is the experimental time scale, and erfc is corresponding to the complementary error function.

Based on the RK theoretical in equation 2.1, the R-K relaxation parameter-dependent of magnetic field $\Gamma(B)$ is given by

$$\Gamma(B) = \frac{\omega_0^4}{8\omega_e D^2} \quad (2.2)$$

where ω_0 is muon electron hyperfine frequency, D is the diffusion rate of electron and ω_e is the electron precision frequency that can be determined from expression.

$$\omega_e = \gamma_e B \quad (2.3)$$

Where γ_e is the electron gyromagnetic ratio. According to equation 2.2, electron diffusion in 1D along the chain, if $\Gamma(B)$ is proportional to $1/B$. This theory was successfully applied to duplicate the electron transfer along the DNA and proteins [55].

2.8 Factors Affecting the Conductivity Measurement in DNA

There are a couple of factors that influenced conductivity in DNA, such as the length, structure, and environment of the DNA molecule. These factors play a significant role and importance to be taken together to understand the electronic charge conductivity of DNA. Due to these factors, different findings of DNA properties (insulator, semiconductor, and conductor) have been proposed by previous studies.

Otsuka et al. [56] and Taniguchi et al. [57] suggested the environmental conditions like humidity would affect the conductivity of the DNA because the ionic conduction through the water layer that surrounded or attached to the DNA would cause the enhancement of conductivity measurement in DNA. The conduction mechanism of DNA was proposed are not due to the electronic conduction of DNA itself but due to the contribution of ionic conduction as well. In addition, DNA found to be more conductive in humid condition rather than dry condition. However, these findings are a bit unclear since the sample was prepared using buffer that made of salt, and the size of the samples also larger. So, there might be a contribution from ion that comes from salt.

In 2014, Wolter et al. [58] have performed density functional theory calculation to study the effect of humidity to the conductivity DNA. From the results, the conductivity of DNA is dependent on humidity because the conductivity has vanished in 37% of humidity, and at high humidity (88% of humidity) the conductivity of DNA is still measurable. Wang also reported that conductivity of DNA is higher in solution rather than in the dry state [59].

In addition to that, Terawaki et al. [34] performed STM measurement on a huge and long double-strand DNA (dsDNA) sample in 0% humidity (dry) and 60% humidity (wet). From the experiment, DNA was found to be not conductive (insulator). This is because the log-current images of DNA did not show any pattern of DNA molecules in the dry condition as shown in Figure 2.11 (a). However, clear images of DNA are obtained in the wet condition. Besides, there is no difference between the I-V characteristic of DNA in the dry condition with the I-V of the mica substrate, as demonstrated in Figure 2.12 (b). This study revealed that the conductivity

measurement of DNA is proposed coming from ionic conduction mechanism in a humid condition [34].

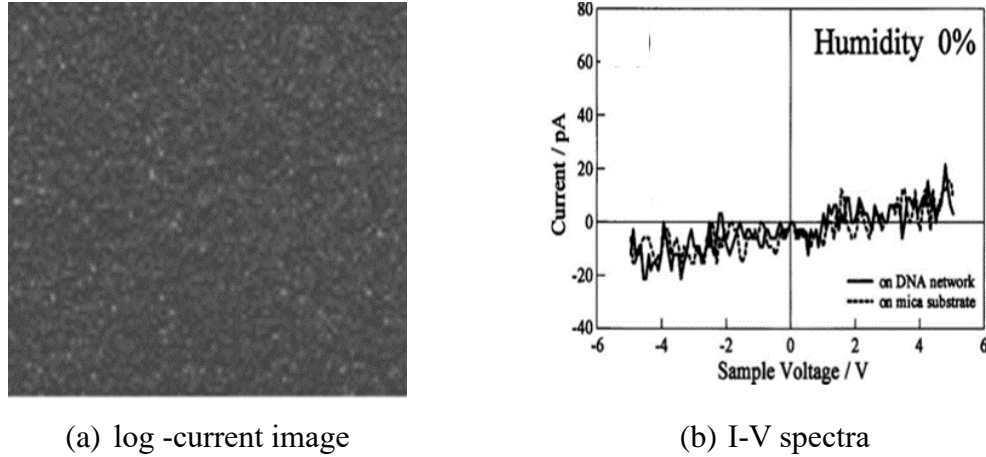


Figure 2.12 Log current imaged and I-V spectra of DNA that was measured under dry condition [38]

On the other hand, Duli et al. [33] studies in 2009 have successfully recorded tunneling current of dsDNA in dry environment. Mechanically controllable break junction (MCBJ) technique has been performed on short dsDNA oligomers that consists of 12 base pairs in a dry condition which surrounded by gas [33].

Besides that, Xu et al. [38] reported the conductivity of DNA in aqueous solution did not significantly contribute by the ionic conduction mechanism. This is because ionic conduction mechanism is insensitive to the changing of the DNA sequence. Both of the samples studies from Xu et al. [38] and Duli et al. [33] were prepared using the salt buffer, and the original structure of the DNA sequences was modified to bind it with the electrode. Ohshiro et al. [46] also succeed to measure the image and STM tip height of ssDNA and dsDNA in a buffer solution. In this study, the conductivity of

In the year 2017, Sharipov et al. [28] have measured the electrical conductivity of DNA molecules using STM. The DNA sample are made of 20-mer oligonucleotide with all ACTG bases. The reagent to synthesis and wash sample contained salt, and a droplet of sample solution was deposited on the gold substrate. The image of the DNA on the gold substrate was successfully observed. Then, the electrical conductivity measurements were performed under the atmosphere condition. Figure 2.12 shows the I-V curve of 20-mer oligonucleotide that was measured in the range of ± 1.5 V bias voltage. According to Figure 2.13, the current-voltage curve that was measured by Sharipov et al. [28] has a similarity with the semiconductor electrical properties.

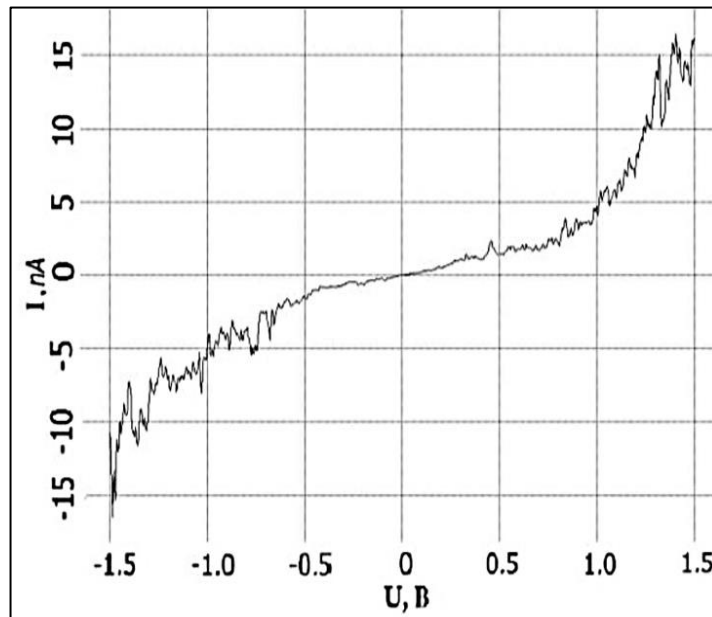


Figure 2.13 I-V characteristic of DNA measured by STM [28].

The similarity for all of these studies by Otsuka et al. [56], Taniguchi et al. [57], Terawaki et al. [34], Xu et al. [38], Duli et al. [33] and Sharipov et al. [28] is the measurements performed on a complex sequence of double-strand DNA. Hence, it was almost impossible to judge which bases in DNA either A, C, T, and G are conductive or non-conductive.

CHAPTER 3

METHODOLOGY

3.1 Introduction

In this study, two main techniques were used to carry out the investigation of electron transport in ssG₁₂, ssC₁₂, ssA₁₂, and ssT₁₂ oligomers. Those techniques are scanning tunneling microscopy (STM) and muon spin spectroscopy (μ SR). The STM technique was used to study the real-space image of the sample surface, the shape and size of the oligomer sample, the tip-height profile, and the current-voltage (I-V) characteristic. In the meantime, the μ SR technique was used to study the characterization of electron motion in each sample and observe the difference of electron motion in each ssDNA₁₂ sample. In this chapter, the details of the experiment for STM *and* μ SR, techniques are presented.

3.2 Scanning Tunneling Microscope

3.2.1 The Working Principle of the STM

STM is an electron microscope that capable to generate real-space images of the sample surface at the atomic level [28, 29, 60]. It was the first instrument for imaging surface with the atomic resolution of 0.01 nm depth resolution and 0.1 nm lateral resolution [44]. The advantage of STM is it could give a true atomic resolution of samples at any condition such as gas, vacuum, and ambient [60]. It is also known as an instrument that extremely sensitive to the local electron density of the sample, and its working principle is based on quantum mechanics [60-62]. This principle allows the electron to tunnel or pass through a potential barrier without touching the surface of the sample and changing the original structure of the DNA sample.

In the STM system, before the STM tip is brought closer to the conductive sample, the gap or distance between the STM tip to the sample surface is larger, and there is no overlapping of electronic wavefunction among them, see the schematic image in Figure 3.1 (a). As the STM tip is brought closer to the sample surface with a distance of about a few Angstrom (0.1-1.0 nm). The electronic wavefunction of the tip overlapped with the wave function of the sample, as shown in Figure 3.1 (b). Once a positive bias voltage (V) is applied to the sample, it caused the Fermi level of tip to push up with respect to the Fermi level of the sample. Accordingly, electron is started to tunnel from the occupied states of the tip to the unoccupied states of the sample, as illustrated in Figure 3.1(b), and measurable current (I) is produced [60]. The amount of current tunneling from tip to the sample is depend on the density of states (DOS) around Fermi energy between tip and sample.

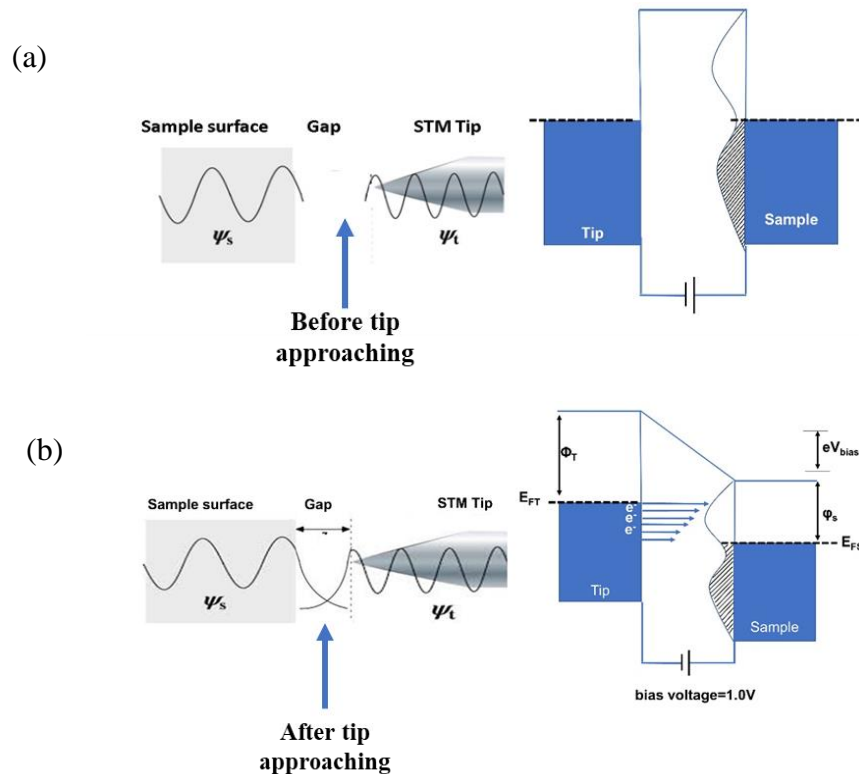


Figure 3.1 Schematic image of the pathway of electron tunneling from the occupied tip states to the unoccupied sample states, (a) before tip approaching the sample, (b) after the tip approaching the sample surface.

The direction of electron tunneling in STM system is depends on the polarity of the sample (sample bias). If the tip is applied with positive bias voltage, electrons tunneling from occupied states of the metallic tip to the unoccupied states of the sample. Thus, the STM image corresponds to the surface map of the filled electronic states of the sample. Meanwhile, when the tip is applied with negative bias voltage, electron tunneling from occupied states of the sample surface to the unoccupied states of the tip [60].

The tunneling current (I) at applied bias V is proportional to the density of states of the sample at energy eV from the Fermi energy, it can be seen from equation 3.1 [60]:

$$I = \int_0^{eV} \rho_t(E) \rho_s(E - eV) T(E, eV) dE \quad (3.1)$$

Where ρ_t and ρ_s represent the local density of states of STM tip and sample.

3.2.2 Operational Mode of STM System

There are two types of operating mode in the STM system: constant height mode and constant current mode [60, 63]. For the constant height mode, the bias voltage and height are both constant. In this mode, the tip is scanning with the same height (h) on the sample surface as demonstrated in Figure 3.2 (a), and the tunneling current will be recorded. It produces an image made of current that changes over the surface, and it can be related to charge density.

On the other hand, for the STM constant current mode, the tip is probing the surface of the sample and maps the details of the charge density of the sample while keeping the current constant. In this mode, the piezoelectric tube controls the tip height

as illustrated in Figure 3.2 (b). Therefore, the topography image will be captured. The images that acquire using constant current mode and constant height mode are called as the topography image and log-current image, respectively.

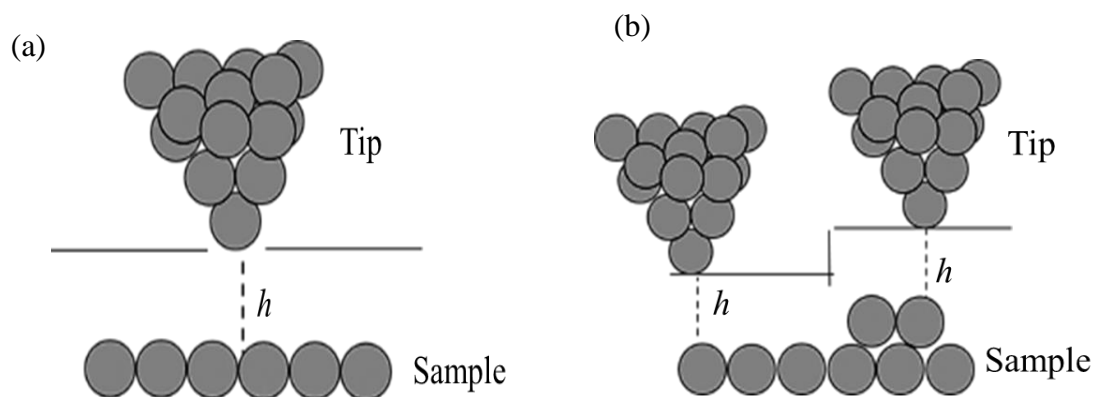


Figure 3.2 Operational modes in the STM system (a) constant height mode (b) constant current mode

3.2.3 Experimental Set-Up and Details

3.2.3(a) Sample Preparation for STM

In this study, the ssA₁₂, ssC₁₂, ssG₁₂, and ssT₁₂ samples were chemically synthesized by Integrated DNA Technologies (IDT) company. The purification of these samples was conducted using the standard desalting method.

For the STM measurements, all the samples of ssDNA₁₂ (ssA₁₂, ssC₁₂, ssG₁₂, and ssT₁₂) were prepared by diluted 0.01 mg of sample powder in 2 mL pure water. These ssDNA₁₂ sample solutions were shaken using an ultrasonic vibrator for about 60 minutes to prevent the molecule structure becomes tangling and attach to each other as demonstrated in Figure 3.3 (a).

At the same time, the STM tip and sample substrate were prepared as well. In STM measurement, the most important part is to create a sharp tip and extremely flat and clean surface of the substrate. The sharp STM tip and clean surface are the key factors to get a good quality image of real structure and an accurate data analysis. In